ASSESSMENT OF OFFSHORE WIND POWER INCLUDING EFFECTS OF SEA SURFACE ROUGHNESS USING OBSERVED WIND STATISTICS

Dag Myrhaug* **and Pål F. Lader**

Department of Marine Technology

Norwegian University of Science and Technology (NTNU)

Trondheim, Norway

***Corresponding author:**

Postal address: Otto Nielsens vei 10, NO-7491 Trondheim, Norway

E-mail address: dag.myrhaug@ntnu.no

Abstract

The paper addresses how the offshore wind power can be assessed based on observed wind statistics at an offshore location. Results are exemplified for a Pierson-Moskowitz wave amplitude spectrum together with mean wind speed statistics from eleven sites in the North Sea and the North Atlantic. The ambient turbulence level, e.g. relevant for design of the wind turbine blades, is also estimated by adopting a wind gust spectrum. The sea surface roughness is specified using a formula given in terms of significant wave height and spectral wave steepness. The present method should be useful for making initial assessments of available wind power and ambient turbulence level at offshore sites based on wind statistics.

Keywords: Offshore wind power; Mean wind speed statistics; Wind gust spectrum; Sea surface roughness.

Introduction

Offshore wind power is an abundant power source which fairly recently has been explored as a promising alternative energy resource. Compared with onshore wind power devices, the engineering community faces increased challenges in designing offshore wind power systems capable of operating and surviving in the harsh environment at sea due to strong winds and additional loads from waves and currents. Bottom fixed structures are commonly used for water depths smaller than about 50 m, while floating wind turbines are installed at larger water depths. A recent comprehensive overview of issues related to offshore wind farms and wind energy is provided by Ng and Ran[1].

The available wind energy for conversion to electrical power depends on the wind speed and the swept area of the wind turbine. A turbine is also specified according to the minimum average wind speed required to start producing power and the shutdown speed above which the turbine is designed to handle (see, e.g. Sasaki[2]; Udoh and Zou[3,4]). The ambient turbulence level associated with the wind conditions is also an issue when designing the wind turbine blades. Thus, an optimum design of a wind power turbine as well as the wind power structure relies on knowledge of the wind field above the sea surface. Kalverla et al.[5] is an example of a recent work performing an extensive analysis of wind conditions in the Dutch part of the southern North Sea. Other studies are those of Udo and Zou[3,4]. Statistical properties of wind conditions for design of offshore wind turbines have also been addressed by, e.g. Li et al.[6] and Horn et al.[7].

The local wind condition above the sea surface is commonly described as the mean wind speed plus the wind gust, i.e. using a logarithmic mean wind speed profile plus a wind gust spectrum (see, e.g. Myrhaug et al.[8]). The sea surface roughness enters in this description of the local wind conditions; it is difficult to estimate depending on air-sea interaction mechanisms which generally should cover the range from small to big waves including wind waves, swell waves, and combined wind waves and swell. Presently, no consistent theory exists covering this wide range of wave conditions. The pioneering work of Charnock[9] was based on a dimensional argument giving the sea surface roughness as $z_0 = \beta u_*^2 / g$ with the original Charnock parameter $\beta = 0.012$, u_* is the friction velocity, and g is the acceleration due to gravity. After that, other values of β as well as z_0 -formulae have been suggested, also including the mean wind speed and the wave age as parameters: see, e.g. Jones and Toba[10], Zhao and Li[11]. Zhao and Li[11] provided a review of the literature up to that date together with their own analysis of both laboratory and field data investigating the influence of wind waves on wind stress in terms of the sea surface roughness and drag coefficient. As in Powell et al.[12] they found that the drag coefficient reaches a peak for strong winds exceeding about 30 – 40 m/s. Zhao and Li[11] also suggested to estimate wind stress from low to high winds using a roughness formula in terms of the spectral wave steepness and the significant wave height (see the next section). Recently, Myrhaug[13] applied this formula to estimate the sea surface roughness based on wind and wave statistics. Other formulations of the sea surface roughness in terms of the spectral wave steepness and the significant wave height have been provided by, e.g. Taylor and Yelland[14] and Takagaki et al.[15] (see the next section). Myrhaug et al.[8] presented some statistical features of the sea surface roughness using the Taylor and Yelland[14] formula together with joint statistics of significant wave height and spectral wave steepness.

The main purpose of this work is to make first assessments of offshore wind power potential and how sensitive it is to sea surface roughness formulations. The analysis is performed using the Takagaki et al.[15] roughness formula in terms of significant wave height and spectral wave steepness referred to together with observed mean wind speed data at eleven offshore locations in the North Sea and the North Atlantic. Moreover, the effect of the sea surface roughness on the ambient turbulence level is also investigated using this roughness formula together with a wind gust spectrum.

This Introduction is followed by giving the theoretical background. The next section provides examples of results for a Pierson-Moskowitz wave amplitude spectrum, observed wind statistics, and the statistical properties of offshore wind power. Then, an assessment of wind gust effects by adopting the Ochi and Shin[16] wind gust spectrum is presented. Finally, summary and conclusions are given. Overall, the presented analytical method provides estimation of offshore wind power based on offshore wind statistics, that can be linked to this energy resource. Thus, it is demonstrated how the present method can be applied to make preliminary assessments of the offshore wind power and the ambient turbulence level at a given site.

Background

Following, e.g. Sasaki[2] the offshore wind power P_w per unit surface area swept by the wind turbine blades is

$$P_w = \frac{1}{2}\rho_a U^3(z) \tag{1}$$

where ρ_a is the air density and $U(z)$ is the horizontal mean wind speed at the elevation z above the sea surface, which commonly is described by the logarithmic profile valid for a neutrally stable atmospheric boundary layer:

$$\frac{U(z)}{U_{10}} = 2.5\sqrt{C_{10}}\, ln\frac{z}{z_0} \tag{2}$$

Here z is positive upwards with $z=0$ at the sea surface, U_{10} is the mean wind speed at $z=10\,\text{m}$, and $C_{10}=(u_*/U_{10})^2$ is the sea surface drag coefficient. Taking $z=10\,\text{m}$ in Eq. (2), C_{10} and z_0 is related by

$$C_{10} = 0.16\,(ln\frac{10}{z_0})^{-2} \tag{3}$$

where z_0 is given in metres.

The sea surface roughness is derived using the formula

$$\frac{z_0}{H_s} = c\, s_p^d \tag{4}$$

where H_s is the significant wave height, $s_p = H_s/((g/2\pi)T_p^2)$ is the spectral wave steepness, T_p is the spectral peak period, c and d are dimensionless coefficients. Here the three following (c, d) values are adopted as proposed by Taylor and Yelland[14], Takagaki et al.[15] and Zhao and Li[11], respectively:

$$(c,d) = (1200, 4.5)\ ,\ TY01 \tag{5}$$

$$(c,d) = (10.94, 3.0)\ ,\ T12 \tag{6}$$

$$(c,d) = (2.79, 2.77)\ ,\ ZL19 \tag{7}$$

The Taylor and Yelland[14] formula was found to be the best to use for mixed wind sea and swell, and for swell-dominant situations for which the spectral wave steepness exceeds 0.02 (but not good for swell dominant conditions with the spectral wave steepness smaller than 0.02). This was concluded by Drennan et al.[17] resulting from performing a comprehensive intercomparison of different parameterizations of the sea surface roughness using field data from eight locations ranging from lakes (two locations in Lake Ontario) to deep water sea (six locations). The Takagaki et al.[15] formula was obtained as a best-fit curve to laboratory and field data for wind speeds ranging up to about 35 m/s and 70 m/s for field and laboratory data, respectively. The Zhao and Li[11] formula was a result of comprehensive analysis of the influence of wind waves on wind stress based on both laboratory and field data. Further details are given in the respective references.

The wind power is commonly evaluated at a specific elevation above the sea surface, i.e. at $z = h$, where the mean wind speed at this elevation can be expressed in terms of U_{10} by using Eqs. (2) and (3), which then substituted in Eq. (1) yields

$$P_W = \frac{1}{2} \rho_a U_{10}^3 \left[\frac{ln(h / z_0)}{ln(10 / z_0)} \right]^3 \tag{8}$$

Examples of results for a Pierson-Moskowitz spectrum and observed wind statistics

Pierson-Moskowitz spectrum

Here the Pierson-Moskowitz (PM) wave amplitude spectrum is chosen since it is directly linked with the mean wind speed, i.e. $H_s = 0.0246\, U_{10}^2$, $T_p = 0.785 U_{10}$ (see Ch. 5.5 in Tucker and Pitt[18]), which gives the spectral wave steepness $s_p = 0.0256$ (i.e. s_p

exceeds 0.02 which was the recommended range for the Taylor and Yelland[14] formula). Substitution of this in Eqs. (4) to (7) yields

$$z_0 = aU_{10}^2 \tag{9}$$

$$a = 2.03 \cdot 10^{-6} \quad , \quad TY01 \tag{10}$$

$$a = 4.52 \cdot 10^{-6} \quad , \ T12 \tag{11}$$

$$a = 2.68 \cdot 10^{-6} \quad , \ ZL19 \tag{12}$$

where a is given in s^2/m. Thus, it appears that the sea surface roughness is largest for T12 followed by ZL19 and TY01. However, there are small differences among the three z_0 formulae as indicated by Eqs. (10) – (12), which is different from the impression as indicated by the significant differences among the three pair values of *c, d* in Eqs. (5) – (7). Thus, the subsequent results will be provided by using the largest (T12) roughness.

Substitution of Eq. (9) in Eq. (8) yields

$$p_w \equiv \frac{P_w}{\rho_a} = \frac{1}{2} U_{10}^3 \left[\frac{ln(h/a) - 2lnU_{10}}{ln(10/a) - 2lnU_{10}} \right]^3 \tag{13}$$

Consequently, the offshore wind power can be estimated for an ocean area from available mean wind speed statistics for the area, for example, from observed wind statistics.

Observed mean wind speed statistics

Here results are provided using eleven cumulative distribution functions (*cdfs*) of U_{10} based on mean wind speed statistics from the North Sea (NS) and the North Atlantic (NA), given by the two-parameter Weibull model

$$P(U_{10}) = 1 - \exp\left[-(\frac{U_{10}}{\theta})^{\beta} \right] \; ; \; U_{10} \geq 0 \qquad (14)$$

The Weibull parameters θ and β are given in Table 1 for four data sets from NS and seven data sets from NA. The data sets are briefly described as follows; further details are provided in the respective references.

One *cdf* of U_{10} is given in Johannessen et al.[19] and is based on 1-hourly values of U_{10} from wind measurements during the years 1973-1999. Four *cdfs* of U_{10} from NA are provided by Mao and Rychlik[20] based on 19 years of wind speed data at four sites along ship routes in NA; the sites with their positions are given in Table 1. Five *cdfs* of U_{10} are provided by Li et al.[6] representing wind speed data from 2001 to 2010; two *cdfs* from NS and three *cdfs* from NA (see Table 1 for more details). One *cdf* of U_{10} from NS (Dogger Bank) is given by Horn et al.[7] based on 60 years of hindcast data.

Statistical properties of offshore wind power

The offshore wind power statistics are estimated by the *cdfs* of U_{10} given in Eq. (14) and Table 1. Relevant statistical quantities are, e.g. the expected (mean) value of P_w, $E[P_w]$, and the variance of P_w, $Var[P_w]$.

Based on the specifications for offshore wind power turbines, the wind power is commonly evaluated within a band of wind speeds, i.e. $U_{10l} \leq U_{10} \leq U_{10u}$. Thus,

$$E\left[p_w(U_{10})\right] = \int_{U_{10l}}^{U_{10u}} p_w(U_{10})\, p(U_{10})\, dU_{10} \tag{15}$$

$$Var\left[p_w(U_{10})\right] = E\left[p_w^2(U_{10})\right] - \left(E\left[p_w(U_{10})\right]\right)^2 \tag{16}$$

where $p_w(U_{10})$ is given in Eq. (13) and $p(U_{10}) = dP(U_{10}) / dU_{10}$ is the probability density function (*pdf*) of U_{10} obtained using Eq. (14).

The present results are exemplified for $h = 90\,\text{m}$, $U_{10l} = 2\,\text{m/s}$, $U_{10u} = 30\,\text{m/s}$ (Udoh and Zou[3]) with $\rho_a = 1.3\,\text{kg/m}^3$. The results for $E\left[P_w\right]$, $E\left[P_w\right]$ + SD and $E\left[P_w\right]$ - SD where SD = $\sqrt{Var\left[P_w\right]}$ is the standard deviation of P_w are provided in Fig. 1 at each site for the T12 z_0 model. It appears that $E\left[P_w\right]$ is largest at site 3 (about 1.8 kW/m^2) followed by those for sites 1, 8, 11, 10, 4, 9, 6, 7, 5 and 2 (about 0.5 kW/m^2), and the standard deviations are large with SD/$E\left[P_w\right]$ ranging from about 1.3 to about 1.9 (at site 10). These different results from site to site reflect the statistical features of U_{10} at the sites (see Table 1).

Assessment of wind gust effects

The effect of wind gust, i.e. the turbulence in the wind field, is also of interest (Udoh and Zou[3,4]). The wind gust is commonly modelled as a Gaussian random process using a wind gust spectrum $S(f)$ with f as the frequency in $Hz = s^{-1}$. Here the horizontal component of the wind gust in the same direction as $U_z = U(z)$ is considered, exemplified adopting the Ochi and Shin[16] wind gust spectrum:

$$S(f_*) = \begin{cases} 583\, f_* & 0 \le f_* \le 0.003 \\ \dfrac{420\, f_*^{0.70}}{(1+f_*^{0.35})^{11.5}} & 0.003 \le f_* \le 0.1 \\ \dfrac{838\, f_*}{(1+f_*^{0.35})^{11.5}} & 0.1 \le f_* \end{cases} \tag{17}$$

where the dimensionless frequency is $f_* = fz / U_z$ and the dimensionless spectrum is $S(f_*) = f\,S(f) / u_*^2$. Here $f\,S(f)$ is the turbulence energy density, which in dimensionless form is

$$\frac{f\,S(f)}{U_{10}^2} = C_{10}\; S(f_*) \tag{18}$$

using $u_*^2 = C_{10} U_{10}^2$.

Fig. 2 shows the turbulence energy density $f\,S(f)$ versus f for the T12 z_0 model at the elevations $z = 10\,\mathrm{m}$ and $z = 90\mathrm{m}$ at two sites with the highest (site 3) and the lowest (site 2) values. The results are qualitatively similar at the other sites. Here $f\,S(f) = U_{10}^2\, C_{10}\, S(f_*)$ with $f = f_* U_{10} / 10$ at $z = 10\,\mathrm{m}$, while at $z = 90\,\mathrm{m}$, $f = f_* U_{90} / 90 = f_* (U_{10} / 90) \cdot 2.5 \sqrt{C_{10}}\, ln(90 / z_0)$ using Eq. (2), and z_0 is taken as

$$E\left[z_0\right] = a\, E\left[U_{10}^2\right] = a \int_{U_{10l}=2m/s}^{U_{10u}=30m/s} U_{10}^2\; p\,(U_{10})\, dU_{10} \tag{19}$$

The maximum values of $f\,S(f)$ using T12 ranges from about 0.13 m^2/s^2 to about 0.40 m^2/s^2. Moreover, as the elevation increases from 10 m to 90 m, the turbulence energy density is shifted from higher to lower frequencies, i.e. there is a shift in the time scale of the turbulence from smaller scales to larger scales as the elevation above the sea surface increases, which qualitatively corresponds to the results provided by Løvseth and Heggem[21] (see also Myrhaug[22]; Myrhaug and Ong[23]).

Finally, the turbulence intensity, $I_z = \sigma_z / U_z$, is evaluated, where $\sigma_z^2 = \int_0^\infty S(f)\,df$. By using Eq. (17) this yields

$$I_z = \frac{U_{10}\sqrt{C_{10}}}{U_z}\left(\int_0^\infty S(f_*)df_*\right)^{1/2} \tag{20}$$

where U_z and C_{10} are given in Eqs. (2) and (3), respectively, and z_0 is taken as in Eq. (19). In neutrally stable maritime boundary layers turbulence is generated mechanically near the sea surface and is dissipated away from the surface, suggesting a general decrease of the turbulence intensity as the elevation increases (Andersen and Løvseth[24]).

Fig. 3 shows the turbulence intensity I_z according to Eq. (20) at 10 m and 90 m for the T12 z_0 model at each site. As expected it appears that the turbulence intensity is larger at 10 m than at 90 m, i.e. with I_{10} and I_{90} in the ranges of about 0.042-0.046 and 0.035-0.038, respectively. Overall, the variation of I_{10} and I_{90} from site to site follows the same trend as depicted in Fig. 1 reflecting the statistical features of U_{10}.

An alternative to this stochastic method is to use a deterministic method for making quick initial assessments of available offshore wind power, that is to use Eq. (1) replacing $U(z)$ with $E\left[U_{10}\right]$, i.e. $E\left[U_{10}\right] = \int_{U_{10l}=2m/s}^{U_{10u}=30m/s} U_{10}\, p(U_{10})\, dU_{10}$, yielding

$$P_{w,\det} = \frac{1}{2}\rho_a \left(E\left[U_{10}\right]\right)^3 \tag{21}$$

Fig. 4 shows the deterministic to stochastic method ratio for the T12 z_0 model at each site. It appears that the ratios are in the range of about 0.39-0.46, i.e. yielding a significantly lower estimate of the available wind power by using the deterministic method than by using the stochastic method. The variation from site to site are due to the statistical features of U_{10}. Overall, the stochastic method should be used as the stochastic features are taken consistently into account, which is not the case using the deterministic method.

Summary and conclusions

This article presents a simple analytical method for estimating the offshore wind power potential based on wind statistics for the mean wind speed 10 m above the sea surface. The ambient turbulence level relevant, e.g. for design of the wind turbine blades is also estimated. Results are exemplified by the Pierson-Moskowitz wave amplitude spectrum together with observed mean wind speed statistics from four sites in the North Sea and seven sites in the North Atlantic. The ambient turbulence level is estimated by the Ochi and Shin[16] wind gust spectrum. The sea surface roughness is represented adopting the Takagaki et al.[15] formula given in terms of significant wave height and spectral wave steepness.

The mean value and the standard deviation of the offshore wind power evaluated 90 m above the sea surface are provided showing that the mean wave power is in the range of about 0.5 kW/m^2 to about 1.8 kW/m^2 with the standard deviation to mean value ratios ranging from about 1.3 to about 1.9. The differences from site to site reflect the statistical features of U_{10} at the sites.

The ambient turbulence level is estimated providing the turbulence energy density and the turbulence intensity evaluated 10 m and 90 m above the sea surface showing that the maximum values of the turbulence energy density range from about 0.13 m^2/s^2 to about 0.40 m^2/s^2. Moreover, the turbulence energy density is shifted from higher to lower frequencies as the elevation increases from 10 m to 90 m, corresponding qualitatively to results presented by Løvseth and Heggem[21]. The turbulence intensity is larger at 10 m than at 90 m, i.e. with the values in the ranges of about 0.042-0.046 and 0.035-0.038, respectively.

Overall, the deterministic to stochastic method ratios are in the range of about 0.39 to 0.46. Thus, the stochastic method should be used to assess the offshore wind power as the stochastic features are taken consistently into account.

The present method should be useful for making initial assessments of the available offshore wind power and the ambient turbulence level at a site based on available wind statistics.

References

1. Ng C, Ran L. Offshore Wind Farms Technologies, Design and Operation. Cambridge, UK: Woodhead Publishing, 2016.
2. Sasaki W. Predictability of global offshore wind and wave power. *Int J Marine Energy* 2017; 17: 98-109.
3. Udoh IE, Zou J. Wind spectral characteristics on strength design of floating offshore wind turbines. *Ocean Systems Eng* 2018; 8(3): 281-312.

4. Udoh IE, Zou J. Wind spectral characteristics on fatigue responses of towerbase and moorings of floating offshore wind turbine. *Ocean Systems Eng* 2019; 9(2): 191-218.
5. Kalverla PC, Steeneveld G-J, Ronda RJ, et al. An observational climatology of anomalous wind events at offshore meteomast IJmuiden (North Sea). *J Wind Eng Ind Aerodyn* 2017; 165: 86-99.
6. Li L, Gao Z, Moan T. Joint distribution of environmental condition in five European offshore sites for design of combined wind and wave energy devices. *ASME J Offshore Mech Arctic Eng* 2015; 137: 031901.
7. Horn J-TH, Krokstad JR, Amdahl J. Joint probability distribution of environmental conditions for design of offshore wind turbines. In: *Proc 36th Int Conf on Ocean Offshore and Arctic Engng*, Trondheim, Norway, 2017, Paper No. OMAE2017-61451.
8. Myrhaug D, Leira BJ, Chai W. Application of a sea surface roughness formula using joint statistics of significant wave height and spectral wave steepness. *J Ocean Eng Marine Energy* 2020; 6: 91-97.
9. Charnock H. Wind stress on a water surface. *QJR Meteorol Soc* 1955; 81: 639-640.
10. Jones ISF, Toba Y. *Wind stress over the ocean*. Cambridge, UK: Cambridge University Press, 2001.
11. Zhao D, Li M. Dependence of wind stress across an air-sea interface on wave states. *J Oceanogr* 2019; 75(3): 207-223.
12. Powell MD, Vickery PJ, Reinhold TA. Reduced drag coefficient for high wind speed in tropical cyclones. *Nature* 2003; 422: 279-283.

13. Myrhaug D. Comments regarding "Dependence of wind stress across on air-sea interface on wave states" by D. Zhao, M. Li. *J Oceanogr* 2020; 76(3): 243-246.

14. Taylor PK, Yelland MJ. The dependence of se surface roughness on the height and steepness of the waves. *J Phys Oceanogr* 2001; 31: 572-590.

15. Takagaki N, Komori S, Suzuki N, et al. Strong correlation between the drag coefficient and the shape of the wind sea spectrum over a broad range of wind speeds. *Geophys Res Letters* 2012; 39: L23604.

16. Ochi MK, Shin YS. Wind turbulent spectra for design considerations of offshore structures. In: *Proc 20th Offshore Tech Conf*, Houston, Texas, 1988, Paper No. 5736 1: 461-467.

17. Drennan WM, Taylor PK, Yelland MJ. Parameterizing the sea surface roughness. *J Phys Oceanogr* 2005; 35: 835-848.

18. Tucker MJ, Pitt EG. *Waves in ocean engineering.* Amsterdam, The Netherlands: Elsevier, 2001.

19. Johannessen K, Meling TS, Haver S. Joint distribution for wind and waves in the Northern North Sea. In: *Proceedings of the 11th offshore and polar engineering conference*, Stavanger, Norway, 2001; 3: 19-28.

20. Mao W, Rychlik I. Estimation of Weibull distribution for wind speeds along ship routes. *Proc IMech E Part M: J Engineering for the Marine Environment* 2017; 231(2): 464-480.

21. Løvseth J, Heggem T. Wind description for coastal and offshore structures. *Concrete under severe conditions 2 Environmental and Loading,* O.E. Gjørv, K. Sakai, N. Banthia, eds, E & FN Spon, London, UK, 1998; 1979-1988.

22. Myrhaug D. Wind gust spectrum over waves: Effect of wave age. *Ocean Eng* 2007; 34(2): 353-358.

23. Myrhaug D, Ong MC. Effect of wave age on wind gust spectra over wind waves. *ASME J Offshore Mech Arctic Eng* 2009; 13(3): 034501.

24. Andersen OJ, Løvseth J. The Frøya database and maritime boundary layer wind description. *Mar Struct* 2006; 19 (2-3): 173-192.

Table 1. Weibull parameters for U_{10} (see Eq. (14)) representing data from the North Sea (NS) and the North Atlantic (NA). Sources: MR[20]; LGM[6]; JMH[19]; HKA[7].

Site	Source	θ (m/s)	β
1. NA: 20° W60° N	MR	10.99	2.46
2. NA: 10° W40° N	MR	7.11	2.30
3. NA: 40° W50° N	MR	11.04	2.48
4. NA: 20° W45° N	MR	9.32	2.47
5. NA: Location 1, Sem Rev	LGM	7.635	2.262
6. NA: Location 3, Buoy Cabo Silleiro	LGM	7.866	2.002
7. NA: Location 5, Wave Hub	LGM	7.859	2.050
8. NS: Location 14, Norway 5	LGM	9.409	2.029
9. NS: Location 15, North Sea Center	LGM	8.920	2.299
10. NS: Northern North Sea	JMH	8.426	1.708
11. NS: Dogger Bank	HKA	9.555	2.220

Figure captions

Fig. 1 $E\left[P_w\right]$, $E\left[P_w\right]$ + SD and $E\left[P_w\right]$- SD where SD = $\sqrt{Var\left[P_w\right]}$ at each site for the T12 z_0 model.

Fig. 2 Turbulence energy density versus frequency at the elevations $z = 10\,\text{m}$ and $z = 90\,\text{m}$ at two sites with the highest (site 3) and the lowest (site 2) values for the T12 z_0 model.

Fig. 3 Turbulence intensity at $z = 10\,\text{m}$ and $z = 90\,\text{m}$ for the T12 z_0 model at each site.

Fig. 4 Deterministic to stochastic method ratio for the T12 z_0 model at each site.

Fig.1

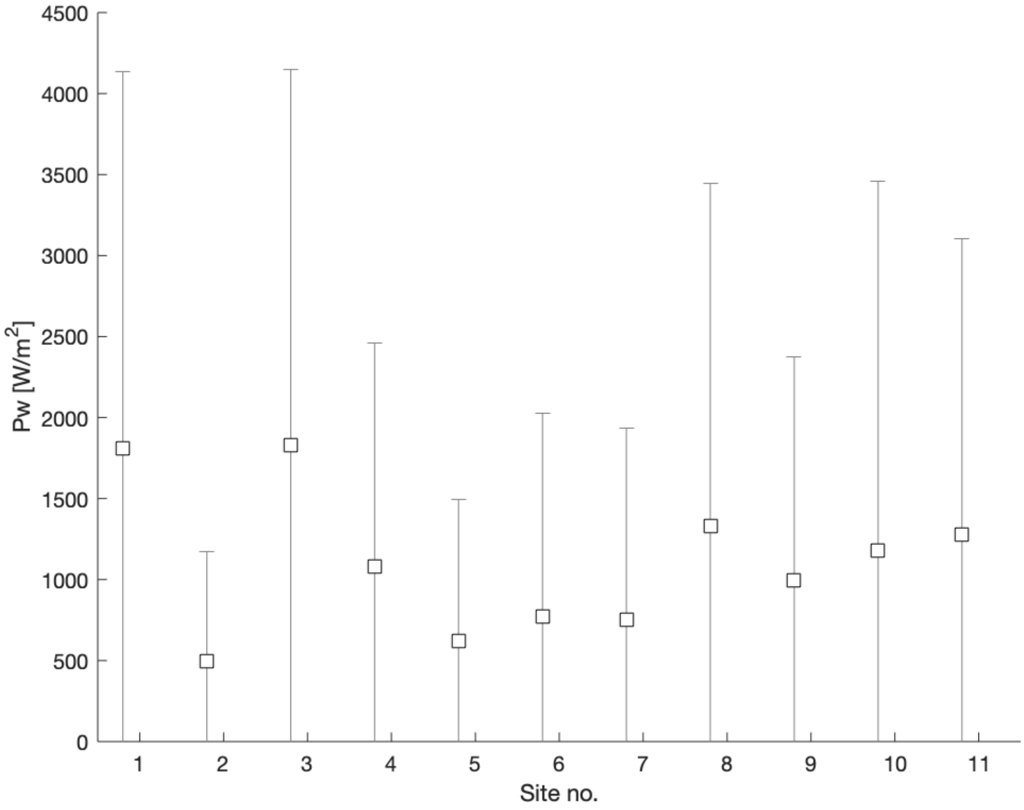

4500
4000
3500
3000
2500
2000
1500
1000
500
0
Pw [W/m2]
1
2
3
4
5
6
7
8
9
10
11
Site no.

Fig. 2

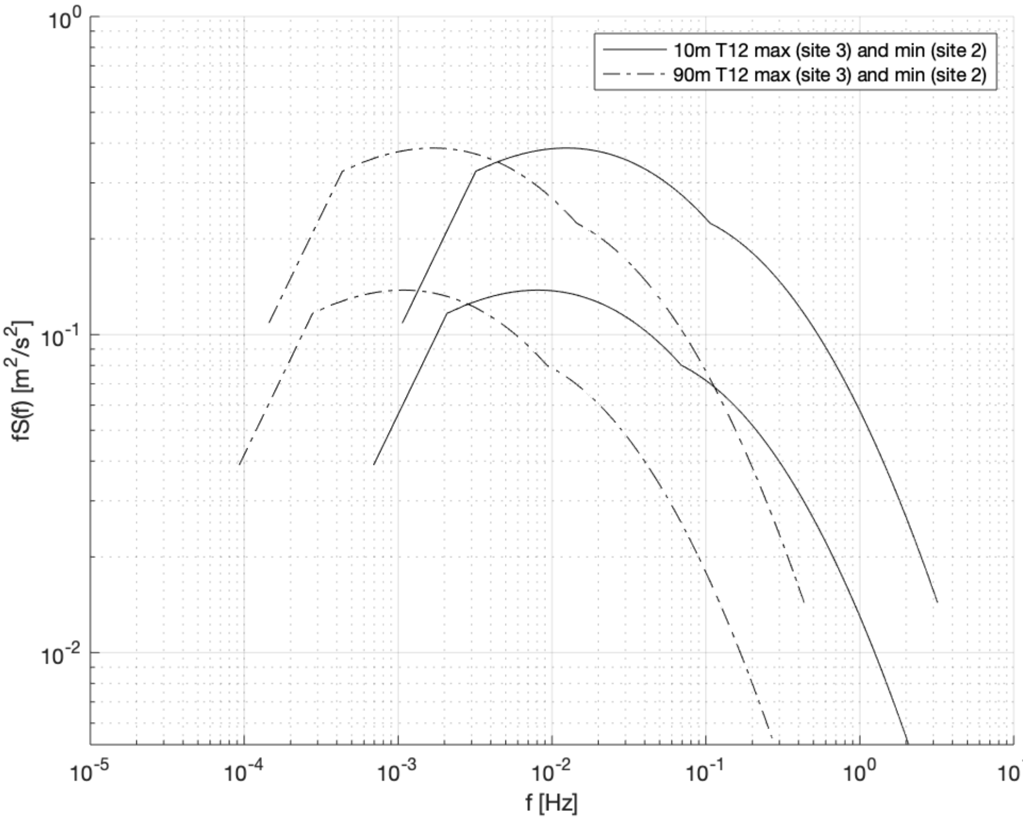

10m T12 max (site 3) and min (site 2)
90m T12 max (site 3) and min (site 2)
fS(f) [m^2/s^2]
f [Hz]
10^0
10^-1
10^-2
10^-5
10^-4
10^-3
10^-2
10^-1
10^0
10^1

Fig. 3

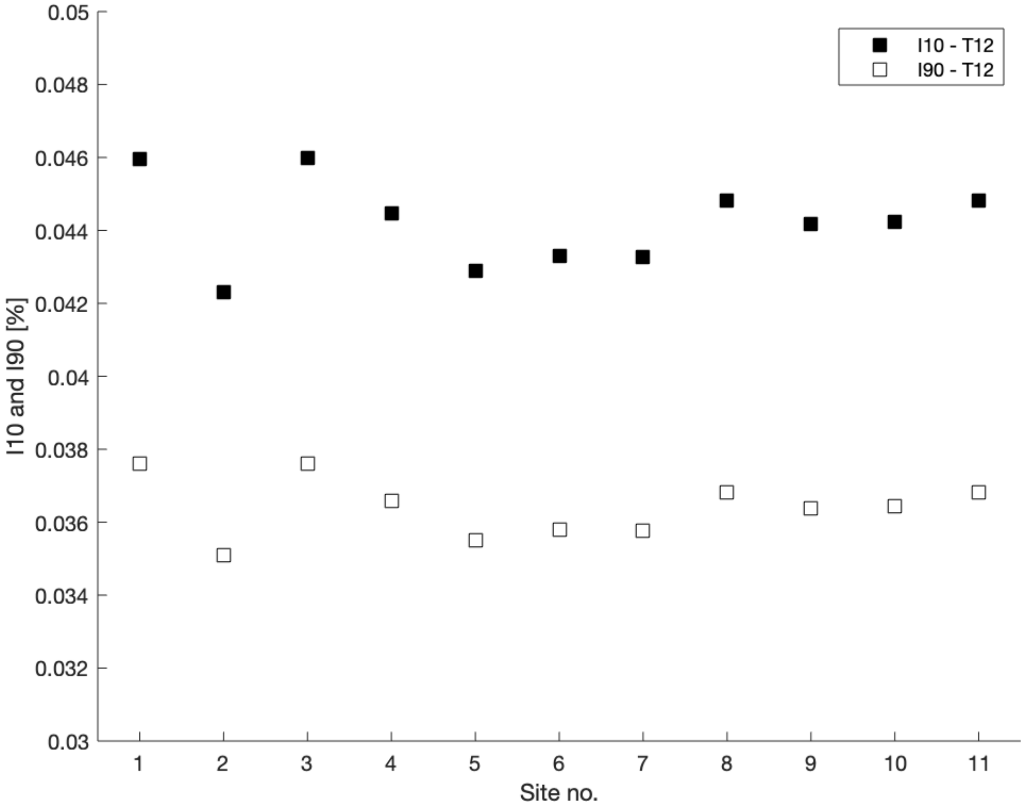

0.05
0.048
0.046
0.044
0.042
0.04
0.038
0.036
0.034
0.032
0.03
I10 and I90 [%]
I10 - T12
I90 - T12
1
2
3
4
5
6
7
8
9
10
11
Site no.

Fig.4

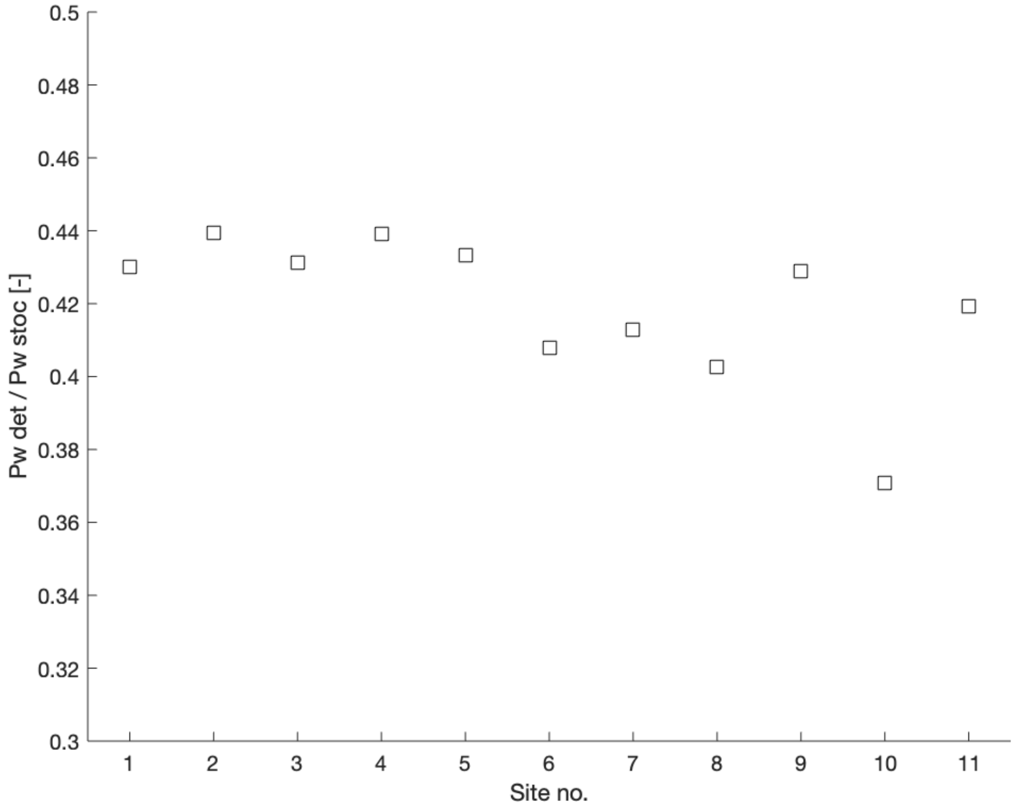

0.5
0.48
0.46
0.44
0.42
0.4
0.38
0.36
0.34
0.32
0.3
Pw det / Pw stoc [-]
1
2
3
4
5
6
7
8
9
10
11
Site no.